Biogeosciences Discuss., 11, 3963–3999, 2014
www.biogeosciences-discuss.net/11/3963/2014/
doi:10.5194/bgd-11-3963-2014

Biogeosciences
Discussions
Open Access

Assessing effects of permafrost thaw on C fluxes based on a multi-year modeling across a permafrost thaw gradient at Stordalen, Sweden

J. Deng[1], C. Li[1], S. Frolking[1], Y. Zhang[2], K. Bäckstrand[3], and P. Crill[3]

[1]Earth Systems Research Center, Institute for the Study of Earth, Oceans and Space, University of New Hampshire, 39 College Road, Durham, NH 03824, USA
[2]Canada Centre for Mapping and Earth Observation, Natural Resources Canada, 588 Booth Street, Ottawa, ON K1A 0Y7, Canada
[3]Department of Geological Sciences, Stockholm University, 106 91 Stockholm, Sweden

Received: 3 February 2014 – Accepted: 26 February 2014 – Published: 11 March 2014

Correspondence to: C. Li (changsheng.li@unh.edu)

Published by Copernicus Publications on behalf of the European Geosciences Union.

Title Page
Abstract | Introduction
Conclusions | References
Tables | Figures
◀| |▶
◀ ▶
Back | Close
Full Screen / Esc
Printer-friendly Version
Interactive Discussion

Title Page
Abstract Introduction
Conclusions References
Tables Figures
◂◂ ▸▸
◂ ▸
Back Close
Full Screen / Esc
Printer-friendly Version
Interactive Discussion

Abstract

Northern peatlands in permafrost regions contain large amount of organic carbon (C) in the soil. Climate warming and associated permafrost degradation are expected to have significant impacts on the C balance of these ecosystems, but the magnitude is uncertain. We incorporated a permafrost model, Northern Ecosystem Soil Temperature (NEST), into a biogeochemical model, DeNitrification-DeComposition (DNDC), to model C dynamics in high-latitude peatland ecosystems. The enhanced model was applied to assess effects of permafrost thaw on C fluxes of a sub-arctic peatland at Stordalen, Sweden. DNDC simulated soil freeze/thaw dynamics, net ecosystem exchange of CO_2 (NEE), and CH_4 fluxes across three typical land cover types, which represent different stages in the process of ongoing permafrost thaw at Stordalen. Model results were compared with multi-year field measurements and the validation indicates that DNDC was able to simulate observed differences in soil thaw, NEE, and CH_4 fluxes across the three land cover types at Stordalen. Consistent with the results from field studies, the modeled C fluxes across the permafrost thaw gradient demonstrate that permafrost thaw and the associated changes in soil hydrology and vegetation increase net uptake of C from the atmosphere, but also increase the radiative forcing impacts on climate due to increased CH_4 emissions. This study indicates the potential of utilizing biogeochemical models, such as DNDC, to predict soil thermal regime in permafrost areas and to investigate impacts of permafrost thaw on ecosystem C fluxes after incorporating a permafrost component into the model framework.

1 Introduction

Northern peatlands are characterized by cold and wet conditions that promote the accumulation of soil organic carbon (SOC) (e.g., Johansson et al., 2006b; Schuur et al., 2008). These ecosystems have accumulated 473–621 Pg (10^{15} g) carbon (C) since the Last Glacial Maximum (Yu et al., 2010), with more than 277 Pg C stored in permafrost areas (Schuur et al., 2008). Although northern peatlands generally acted as sinks of carbon dioxide (CO_2) in the past and under current climate (e.g., Lund et al., 2010; McGuire et al., 2009); these C stocks may be released to the atmosphere with climate warming, due to mobilization of previously frozen C in permafrost soils and accelerated decomposition of SOC (e.g., Frolking et al., 2011; McGuire et al., 2009; Schuur et al., 2009, 2011). In addition, because of prevailing anaerobic soil conditions, northern peatlands are an important source of atmospheric methane (CH_4), releasing 31–65 $\mathrm{Tg\,CH_4\,yr^{-1}}$ (McGuire et al., 2009).

Pronounced warming has been observed in northern high latitudes, with surface air temperature increased by approximately 0.09 °C $\mathrm{decade^{-1}}$ during the 20th century (ACIA, 2005). More pronounced warming has been projected at this region for the 21st century (IPCC, 2007). As a result of climate warming, degradation of permafrost has been documented in northern peatlands (e.g., Christensen et al., 2004; Payette et al., 2004; Åkerman and Johansson, 2008). Permafrost thaw can result in increases in active layer thickness (ALT; the thickness of surface soil layer that freezes and thaws seasonally above a year-round frozen layer) and cause land surface subsidence, which in turn may cause changes in topography, soil hydrology, and vegetation (e.g., Avis et al., 2011; Johansson et al., 2006a; Schuur et al., 2008). These changes associated with permafrost degradation can significantly affect C cycle in northern ecosystems (e.g., Dorrepaal et al., 2009; Johansson et al., 2006b; McGuire et al., 2009; Schneider von Diemling et al., 2012).

Although much concern has been placed on C balance in permafrost ecosystems, large uncertainty still exists (e.g., Koven et al., 2011; McGuire et al., 2009; Schuur et al., 2011). Northern peatlands are highly heterogeneous, usually with varying characteristics of permafrost, topography, hydrology, soil, and vegetation within close proximity (Nungesser, 2003), which results in considerable variations of C fluxes at local and landscape scales (e.g., Bäckstrand et al., 2010; Lund et al., 2010; Sachs et al., 2010). Responses of C balance to permafrost degradation have been shown to vary across different peatlands as well (Bäckstrand et al., 2010). Therefore, it is an ongoing challenge to extrapolate site-specific measurements to large regions.

Process-based models are effective tools to assess the impacts of climate change on boreal ecosystems. Several large-scale models have been enhanced by incorporating thermal, hydrologic, vegetation, and biogeochemical processes in relation to permafrost conditions (e.g., Schneider von Diemling et al., 2012; Wania et al., 2009a, 2009b; Zhuang et al., 2001, 2004). These models have been applied to quantify the impacts of climate change on C fluxes at regional and global scales (e.g., Schneider von Diemling et al., 2012; Wania et al., 2009a, 2009b; Zhuang et al., 2001, 2004, 2006). Predictions by large-scale models are generally done at coarse spatial resolutions, therefore disregarding the effects of local spatial heterogeneity. By ignoring fine-scale spatial heterogeneity in vegetation and environmental conditions, systematic biases may occur in simulations of permafrost degradation and C fluxes (Bohn and Lettenmaier, 2010; Zhang et al., 2013). In addition, the results based on coarse-scale modeling are difficult to validate by comparing with field observations and uncertainty may be resulted in regional and global simulations due to limited validation (Kirschke et al., 2013).

A process-based biogeochemical model, DeNitrification-DeComposition (DNDC), was recently enhanced by incorporating a permafrost model, Northern Ecosystem Soil Temperature (NEST), for predicting biogeochemistry in high latitudes from plant communities to ecosystem scale. The model was initially tested against one growing season of CH_4 flux data measured at a permafrost site in the Lena River Delta, Russia (Zhang et al., 2012). In this study, we applied the enhanced model to assess effects of permafrost thaw on C fluxes of a sub-arctic peatland at Stordalen, Sweden. DNDC simulated multi-year soil freeze/thaw dynamics, net ecosystem exchange of CO_2 (NEE), and CH_4 fluxes across three typical land cover types, which represent different stages of permafrost degradation in the study region. The model was tested against long-term field measurements to verify its applicability for simulating the differences in soil thermal regime and C fluxes across a gradient of permafrost thaw. Then we assessed the possible impacts of permafrost thaw on C fluxes for the Stordalen peatland based on the multi-year simulations.

2 Methods and data

2.1 The study area and field observations

The study area is the Stordalen mire (68°20′ N, 19°03′ E, 351 m a.s.l.) located 10 km southeast of Abisko Scientific Research Station (ANS) in northern Sweden. It is a subarctic peatland with discontinuous permafrost. This area has a continental climate, with an annual mean air temperature of 0.07 °C and an average annual precipitation of 308 mm during 1986–2006 according to the observations at ANS (Callaghan et al., 2010). Long-term climate records at ANS indicated that the annual mean air temperature in this region has increased by 2.5 °C from 1913 to 2006, significantly exceeding the 0 °C threshold for the first time during the last few decades (Bäckstrand et al., 2008; Callaghan et al., 2010). This warming has led to a thicker active layer and permafrost disappearance in this area (Åkerman and Johansson, 2008). The degradation of permafrost has significantly affected surface topography, local hydrology, vegetation, and subsequently exerted a strong influence on the fluxes of CO_2 and CH_4 (Christensen et al., 2004; Johansson et al., 2006b; Malmer et al., 2005; Åkerman and Johansson, 2008).

As in most peatlands in permafrost regions, Stordalen mire has high spatial heterogeneity in topography (1–2 m relative differences in elevation). The variability of topography creates small-scale (meters) environments with different soil moisture and nutrient conditions that support different plant communities (Rosswall et al., 1975; Bäckstrand et al., 2008). The area can be classified into three typical land cover types (i.e., dry *Palsa*, mesic *Sphagnum*, and wet *Eriophorum*), which differ in their permafrost regime, soil water condition, and vegetation composition (Bäckstrand et al., 2008, 2010). During the last three decades, there have been pronounced shifts in the extent of these three land cover types, with *Palsa* sites being converted into *Sphagnum* sites or *Eriophorum* dominated sites (Christensen et al., 2004; Malmer et al., 2005). These three land cover types can be regarded as representing different stages of permafrost degradation (e.g., Malmer et al., 2005; Johansson et al., 2006b; Bäckstrand et al., 2010).

CO_2 and CH_4 fluxes have been measured using automated chambers at Stordalen during 2003 to 2009. NEE was measured at three sites (i.e., the *Palsa*, *Sphagnum*, and *Eriophorum* sites) to represent three typical land cover types, and CH_4 emissions were consistently observed at the *Sphagnum* and *Eriophorum* sites, where water table levels were over or near the peat surface (Bäckstrand et al., 2008, 2010) (the sign convention is that positive values represent net CO_2 or CH_4 emissions into the atmosphere and negative fluxes represent net CO_2 or CH_4 uptake). The *Palsa* site is relatively dry and its CH_4 flux is near zero (Bäckstrand et al., 2008). For each chamber, auto-chamber system measured CO_2 and total hydrocarbon (THC) fluxes every three hours and there were eight measurements per day. CH_4 fluxes were manually observed approximately three times per week by taking samples from every chamber and these measurements were used to quantify the proportion of CH_4 in the measured THC (Bäckstrand et al., 2008, 2010). Daily NEE and CH_4 fluxes were calculated as average values of eight measurements. During 2003 to 2009, valid rates of daily NEE were calculated for 85–213 days in a year based on the field measurements. Daily CH_4 fluxes were available for 79–116 days in a year, with an exception in 2006 when the instrument was down (Bäckstrand et al., 2008, 2010). In addition, soil thaw depth (measured to 90 cm) and water table depth (WTD) were measured 3–5 times per week from early May to mid October each year (Bäckstrand et al., 2008). Daily meteorological data, including air temperature, precipitation, solar radiation, wind speed, as well as relative humidity, were recorded at the ANS (Fig. 1). The technical details regarding the measurements of NEE and CH_4 fluxes, and the relevant auxiliary variables were described by Bäckstrand et al. (2008, 2010).

2.2 Modification of DNDC

2.2.1 Overview of the DNDC model

DNDC is a process-based model developed for quantifying C sequestration as well as the emissions of carbon and nitrogen (N) gases from terrestrial ecosystems (Li et al., 1992a, 1992b, 2000; Stange et al., 2000; Zhang et al., 2002). The model has incorporated a relatively complete suite of biophysical and biogeochemical processes, which enables it to compute the complex transport and transformations of C and N in terrestrial ecosystems under both aerobic and anaerobic conditions.

DNDC is comprised of six interacting sub-models: soil climate, plant growth, decomposition, nitrification, denitrification, and fermentation. The soil climate, plant growth, and decomposition sub-models convert the primary drivers, such as climate, soil properties, vegetation, and anthropogenic activity, into soil environmental factors, such as soil temperature and moisture, pH, redox potential (Eh), and substrate concentrations. The nitrification, denitrification, and fermentation sub-models simulate C and N transformations that are mediated by soil microbes and controlled by soil environmental factors (Li, 2000; Li et al., 2012). In DNDC, NEE is calculated as the difference between net primary production (NPP) and soil microbial heterotrophic respiration (HR). NPP is simulated at daily time step by considering the effects of several environmental factors on plant growth, including radiation, air temperature, soil moisture, and N availability. The model simulates the production of plant litter and incorporates the plant litter into pools of soil organic matter (SOM). HR is calculated by simulating decomposition of SOM. SOM is divided into four pools in DNDC, namely litter, microbes, humads, and passive humus. Each pool is further divided into two or three sub-pools with specific C to N (C/N) ratios and decomposition rates. As a microbially-mediated process, decomposition of each SOM fraction depends on its specific decomposition rate as well as soil thermal and moisture conditions (Li et al., 2012). Methane flux is predicted by modeling CH_4 production, oxidation, and transport processes. CH_4 production is simulated by tracking a series of reductive reactions between electron donors (i.e., H_2

and dissolved organic carbon) and acceptors (i.e., NO_3^-, Mn^{4+}, Fe^{3+}, SO_4^{2-}, and CO_2). In DNDC, CH_4 production and oxidation can occur simultaneously within a soil layer but within relatively aerobic and anaerobic micro-sites, whose volumetric fractions are defined by an Eh calculator, a so-called "anaerobic balloon", embedded in the model framework (Li, 2007). Redox potential, temperature, pH, along with the concentrations of electron donors and acceptors are the major factors controlling the rates of CH_4 production and oxidation. CH_4 is transported from soil into atmosphere via plant-mediated transport, ebullition, and diffusion (Fumoto et al., 2008; Zhang et al., 2002).

2.2.2 Soil freeze/thaw and permafrost dynamics

Traditionally, DNDC simulated soil thermal dynamics by a relatively simple module without detailed processes describing the soil thermal regime in the presence of permafrost. It did not explicitly simulate energy exchange within soil-vegetation-atmosphere system, snowpack thermal dynamics, the presence of permafrost, as well as active layer dynamics (Zhang et al., 2002). However, these processes or environmental factors are important for characterizing the permafrost regime, soil thermal dynamics, soil hydrology, as well as C and N cycles in high latitudes (e.g., Riseborough et al., 2008; Waelbroeck, 1993). In order to make DNDC more suitable for northern ecosystems, especially frozen soil conditions, we incorporated a permafrost model, NEST, into the model framework (Zhang et al., 2012). NEST is a process-based model which simulates ground thermal dynamics, soil freeze/thaw dynamics, and permafrost conditions (Zhang et al., 2003). In NEST, soil temperature and permafrost thermal regime are calculated by solving the heat conduction equation, with the upper boundary condition determined by surface energy balance and the lower boundary condition being defined as geothermal heat flux. The effects of climate, vegetation, snow pack, ground features, and hydrological conditions on soil thermal regime are incorporated into the model on the basis of energy and water exchanges within soil-vegetation-atmosphere system (Zhang et al., 2003, 2005). After coupled to NEST, DNDC was able to simulate both the seasonal dynamics of active layer and the long-term variations of permafrost and their effects on biogeochemical processes (Zhang et al., 2012).

2.3 Model application

We performed DNDC simulations for the three typical land cover types (*Palsa*, *Sphagnum*, and *Eriophorum*) from 2002 to 2009. Daily meteorological data (i.e., maximum, mean, and minimum air temperature, precipitation, solar radiation, wind speed, and humidity) from 2002 to 2009 recorded at the ANS were collected to support the simulations. All sites had a surface soil layer of peat (0.5 m) overlying a silt soil layer (Rosswall et al., 1975; Rydeñ et al., 1980; Olefeldt et al., 2012). The peat had a bulk density of $0.15\,\mathrm{g\,cm^{-3}}$, SOC content of $0.5\,\mathrm{kg\,C\,kg^{-1}}$ SDW (soil dry weight), total porosity of 0.9, field capacity of 0.4 (water-filled pore space), wilting point of 0.15 (water-filled pore space), and pH (H_2O) of 5.0, according to observations from Malmer and Walleñ (1996), Rydeñ et al. (1980), and Öquist and Svensson (2002). The local bedrock is granite (Rosswall et al., 1975) and a thermal conductivity of $2.9\,\mathrm{W\,m^{-1}\,{}^{\circ}C^{-1}}$ was used (Clauser and Huenges, 1995). The geothermal heat flux in the study region was estimated as $0.06\,\mathrm{W\,m^{-2}}$ (Majorowicz et al., 2011).

While the three land cover types share common conditions regarding weather, geology, and soil during the simulations, they differ in soil hydrologic conditions and vegetation characteristics. In order to predict the dynamics of water table at the *Sphagnum* and *Eriophorum* sites, DNDC used several parameters to estimate lateral flows, including surface inflow rate, maximum water table depths for surface and ground outflows, as well as surface and ground outflow rates (Zhang et al., 2002). We estimated these parameters by comparing the modeled and observed WTD (Table 1). To reduce the influences of prediction-error of WTD on soil thermal and biogeochemical processes, the observed WTDs were used during the simulations if the measurements were available. For the *Palsa* site, we assumed that there is no surface lateral inflow and water will flow away each day when the water table is above the land surface or water infiltrates into frost table, based on local studies (Rydeñ et al., 1980). DNDC also requires phenological and physiological parameters to simulate plant growth, including maximum biomass production and its partitioning to shoot and root, vegetation C/N ratio, required thermal degree days for vegetation growth, plant water requirement, and an index of biological N fixation. These parameters for the three land cover types were determined either based on literature or as model defaults (Table 2).

To initialize the soil climate conditions, the soil thermal and hydrological modules of DNDC were iteratively ran by using the climate data in 2002 until the simulated annual mean soil temperature was stable. Then the vegetation and soil biogeochemical modules were activated and the model was run continuously from 2002 to 2009. We validated the model by using the measured soil thaw depth, NEE, and CH_4 fluxes. Two statistical indexes, the relative root mean squared error (RMSE, Eq. 1) and the coefficient of correlation (R, Eq. 2), were used to quantity the accordance and correlation between model predictions and field observations (Moriasi et al., 2007).

$$\mathrm{RMSE} = \frac{100}{|\overline{o}|}\sqrt{\frac{\sum_{i=1}^{n}(p_i - o_i)^2}{n}} \tag{1}$$

$$R = \frac{\sum_{i=1}^{n}(o_i - \overline{o})(p_i - \overline{p})}{\sqrt{\sum_{i=1}^{n}(o_i - \overline{o})^2 \sum_{i=1}^{n}(p_i - \overline{p})^2}} \tag{2}$$

In both equations, o_i and p_i are the observed and simulated values, respectively; $\overline{o}$ and $\overline{p}$ are their averages; and n is the number of values.

To quantify the differences of C fluxes for the three land cover types across permafrost thaw gradient, the simulated annual NEE and CH_4 fluxes form 2003 to 2009 were collected for analysis. The CH_4 fluxes from dry *Palsa* were assumed to be zero (Bäckstrand et al., 2008). We calculated net emissions of greenhouse gases (GHG) for the three land cover types as CO_2-equivalents by using a 100-year global warming potential (GWP) of 25 kg CO_2-equivalents kg^{-1} CH_4 (IPCC, 2007). In addition, we estimated the possible impacts of permafrost thaw on C fluxes and GHG emissions for the

Stordalen mire based on the model results and changes in the fractions of the three land cover types from 1970 to 2000.

3 Results and analyses

3.1 Model validation

3.1.1 Thaw depth

Figure 2 shows the seasonal dynamics of the observed and simulated thaw depth during 2003 to 2009. As field observations demonstrate, thaw rates varied across the three land cover types. At the *Palsa* site, the maximum thaw depth usually ranged from 45 to 60 cm during the summer seasons from 2003 to 2009; while the soil was often thawed to greater than 90 cm by August or September at the *Sphagnum* site and by June or July at the *Eriophorum* sites. Therefore, the thaw rates were relatively slow, moderate, and rapid at the *Palsa*, *Sphagnum*, and *Eriophorum* sites, respectively. In comparison with the observations, the DNDC model generally captured the differences of thaw depth across the three land cover types as well as their seasonal dynamics (Fig. 2). The simulations showed that the dry *Palsa* site had an active layer thickness of around 55 cm. The thaw depth reached deeper than 100 cm by the end of July to September at the mesic *Sphagnum* site and by June or July at the wet *Eriophorum* site.

The model results demonstrated that rate of summer thaw accelerated along the gradient of soil moisture. The different soil thaw rates in the DNDC simulations were mainly induced by the various values of thermal conductivity resulting from the differences of soil water conditions across the three sites. This explanation is consistent with the conclusion based on the local field study (Rydén and Kostov, 1980). However, few discrepancies remained between the modeled and observed results, primarily in the soil thaw dynamics at the *Sphagnum* site, where DNDC overestimated the thaw rate during the late periods of soil thaw in 2003 and 2006 (Fig. 2h and k), although it captured the seasonal variations in other years. Nevertheless, the comparisons between the simulations and observations indicated that DNDC can reliably predict differences in the dynamics of soil thaw at the three land cover types at Stordalen, which is crucial for correctly simulating the impacts of permafrost thaw on soil hydrology, plant growth, and biogeochemical processes.

3.1.2 NEE

Figure 3a–g illustrates the observed and simulated daily NEE at the *Palsa* site. The daily observations were highly variable and showed a clear seasonal cycle across 2003 to 2009, with net CO_2 uptake increasing in early summer, CO_2 uptake most days during mid-summer and net CO_2 emissions in late summer and autumn. In comparison with the measurements, DNDC generally captured the magnitude and seasonal characteristics of daily NEE, although discrepancies existed. The R values were calculated for each year and ranged from 0.40 to 0.69 (Fig. 3a–g), indicating that there were significant correlations between the simulated and observed daily NEE in each year ($P < 0.0001$). Table 3 lists the observations and simulations on the cumulative NEE for the seven growing periods from 2003 to 2009. The observed cumulative NEE ranged from −435 to −241 kg CO_2-C ha^{-1} and the modeled values ranged from −414 to −265 kg CO_2-C ha^{-1}. The calculated RMSE values varied between 3 % and 25 % (mean: 13 %) across the seven growing seasons (Table 3), which indicates that DNDC successfully simulated the cumulative NEE during growing seasons.

At the *Sphagnum* site, the DNDC model generally captured the variations of daily NEE over 2004 to 2009 (Fig. 3i–n). However, discrepancies appeared in 2003. For example, the field observations showed high net uptake rates of CO_2 during 25 May to 22 June in 2003; while the model predicted lower rates (Fig. 3h), primarily because of low solar radiation and air temperature (the mean was 6.0 °C during 25 May to 22 June) limitations on plant productivity. Nonetheless, the modeled and observed daily NEE were significantly correlated in all years ($P < 0.001$ in 2003 and $P < 0.0001$ in other years), with R values ranged from 0.35 to 0.79 (Fig. 3h–n). The predicted cumulative NEE ranged from −521 to $-203\,\mathrm{kg\,CO_2-C\,ha^{-1}}$ over seven growing seasons. The results are consistent with the corresponding observations, ranging from −525 to $-212\,\mathrm{kg\,CO_2-C\,ha^{-1}}$ (Table 3). The values of RMSE ranged from 1 % to 17 % with a mean of 6 % over 2003 to 2009 (Table 3).

At the *Eriophorum* site, DNDC also successfully predicted the seasonal patterns of daily NEE, displaying good agreement between the simulations and observations (Fig. 3o–u). The R values ranged from 0.39 to 0.74, which indicates significant ($P < 0.0001$) correlations between the modeled and measured daily NEE in each year during 2003 to 2009. At the *Eriophorum* site, the observed daily uptake rates of CO_2 were usually higher than that at the *Palsa* and *Sphagnum* sites during summer (Fig. 3). The DNDC model captured the differences across these three sites and the magnitudes of the simulated NEE were comparable with the corresponding observations. The simulations of growing season cumulative NEE ranged from −1078 to −365 kg CO_2-C ha^{-1} during 2003 to 2009, which were close to the observations (ranged from −1118 to −270 kg CO_2-C ha^{-1}), The RMSE values ranged from 1 % to 35 % (mean: 15 %) over 2003 to 2009 (Table 3). The comparison demonstrates that DNDC reliably simulated the growing season cumulative NEE at the *Eriophorum* site.

3.1.3 Water table and CH_4 fluxes

In this study, water table was simulated for the days without field observation; otherwise the observed water table was used to determine the soil water conditions. As shown by Fig. 4a–g, WTDs (with positive values for above-ground and negative values for belowground) fluctuated between −30 to 0 cm at the *Sphagnum* site, while were generally near or above the ground surface at the *Eriophorum* site.

Figure 4h–n compares the observed and simulated daily CH_4 fluxes at the *Sphagnum* site. DNDC generally matched the observed daily CH_4 fluxes in both magnitudes and seasonal characteristics during the six studied years from 2003 to 2009 (excluding 2006), despite few inconsistencies remained. The modeled results indicated that the temporal patterns of CH_4 fluxes were primarily controlled by the changes of WTD and soil temperature at the *Sphagnum* site. The R value ranged between 0.63 and 0.89 over the six years (Fig. 4h–n), which indicates significant correlations between the simulated and observed daily CH_4 fluxes in each year ($P < 0.0001$). Of the six tested sampling periods, the simulations of cumulative CH_4 fluxes varied from 12.7 to 35.7 $\mathrm{kg\,CH_4-C\,ha^{-1}}$, which were comparable with the observations (varied from 9.7 to 30.6 $\mathrm{kg\,CH_4-C\,ha^{-1}}$, Table 4). The values of RMSE ranged from 4 % to 35 % with a mean of 21 % (Table 4).

At the *Eriophorum* site, DNDC also approximately matched the observed daily CH_4 fluxes over the six studied years from 2003 to 2009 (excluding 2006; Fig. 4o–u). However, few biases still existed. For instance, DNDC underestimated the magnitudes of CH_4 fluxes in 2008 and had a relatively later onset of emissions than observations (Fig. 4t). Nonetheless, the correlations between the modeled and measured daily CH_4 fluxes were statistically significant ($P < 0.0001$) in each year, with R values ranging from 0.47 to 0.89 over the six years. The modeled results demonstrated that the temporal patterns of CH_4 fluxes at the *Eriophorum* site were mainly related to the changes in soil temperature and the associated variations of plant growth and soil decomposition, because of the inundated conditions at this site. This conclusion is consistent with the field results (e.g., Bäckstrand et al., 2008; Jackowicz-Korczyñski et al., 2010). As illustrated by Fig. 4h–u, the observed daily CH_4 fluxes at the *Eriophorum* site were generally higher than that at the *Sphagnum* site. DNDC well captured the differences between these two sites. Of the six tested sampling periods, the observed cumulative CH_4 fluxes ranged from 57.9 to 121 $\mathrm{kg\,CH_4-C\,ha^{-1}}$, while the modeled results varied from 45.5 to 113 $\mathrm{kg\,CH_4-C\,ha^{-1}}$. The RMSE values ranged from 3 % to 22 % with a mean of 12 % across these six periods (Table 4), which indicates a good accordance between the simulations and observations of CH_4 fluxes.

3.2 Annual C fluxes and GHG

In this section, we review simulated annual (not growing season) NEE and CH_4 fluxes at the *Palsa*, *Sphagnum*, and *Eriophorum* sites from 2003 to 2009. The simulated annual total NEE varied from −132 to 56.5 (*Palsa*; mean: −50.9), −492 to −191 (*Sphagnum*; mean: −342), and −1021 to −399 (*Eriophorum*; mean: −793) kg CO_2-C $ha^{-1}\,yr^{-1}$, and inter-annual variability of NEE increased with increasing magnitude (Fig. 5a). The predictions of annual total NEE were different across the *Palsa*, *Sphagnum*, and *Eriophorum* sites and primarily resulted from differences in environment conditions, including soil temperature, thaw regime, soil moisture content, and vegetation characteristics, across these three land cover types. DNDC predicted the highest uptake rates of CO_2 at the *Eriophorum* site, primarily due to (1) the highest value of the maximum productivity under optimum growing conditions (Table 2); (2) the fastest soil thaw rate (Fig. 2), which was favorable for water and nitrogen uptake; and (3) a permanently high water table (Fig. 4a–g) which restricted soil heterotrophic respiration and provided abundant water for plant transpiration. The lowest rates of annual total NEE were simulated at the *Palsa* site, primarily because of (1) the lowest value of the maximum productivity under optimum growing conditions (Table 2), (2) the slowest soil thaw rate and limited summer thaw depths (Fig. 2), and (3) a relatively dry soil which restricted plant transpiration and was comparatively favorable for soil decomposition.

During 2003 to 2009, the simulations of annual total CH_4 fluxes ranged from 17.9 to 42.2 (*Sphagnum*; mean: 32.8) and 72.2 to 125 (*Eriophorum*; mean: 104) kg CH_4-C $ha^{-1}\,yr^{-1}$. As with NEE simulations, inter-annual variability of CH_4 fluxes increased with increasing annual means (Fig. 5a). The annual total CH_4 fluxes were different across the *Sphagnum* and *Eriophorum* sites (Fig. 5a). Simulated CH_4 fluxes were higher at the *Eriophorum* site than the *Sphagnum* site due to: (1) increased rates of CH_4 production due to higher soil temperature and faster thaw rate, (2) a higher water table that supported CH_4 production while restricting CH_4 oxidation, (3) higher plant growth rates and consequently more substrates (e.g., CO_2 and dissolved organic carbon) used for CH_4 production, and (4) accelerated rates of CH_4 transport due to increased plant vascularity.

Annual net C fluxes were calculated as the sum of annual total NEE and CH_4 fluxes in this study (i.e., horizontal loss of dissolved organic carbon was not considered). Because the CH_4 component was assumed to be zero at the *Palsa* site, the simulated annual net C fluxes were equal to annual NEE (range: −132 to 56.5 kg C ha^{-1}, mean: −50.9 kg C ha^{-1}) at this site. Simulations of annual net C fluxes ranged between −462 to −163 (mean: −309) and −934 to −488 (mean: −689) kg C ha^{-1} at the *Sphagnum* and *Eriophorum* sites, respectively, during 2003 to 2009. These results illustrated that C uptake rates increased along the permafrost thaw gradient at Stordalen (Fig. 5b). Net GHG emissions, expressed as CO_2-equivalents, were calculated by considering more powerful radiative forcing potential of CH_4 than CO_2 (25 times over a 100-year horizon). The simulated annual GHG at the *Palsa* site varied from −485 to 207 kg CO_2-eq. ha^{-1} yr^{-1}, with a mean of −186 kg CO_2-eq. ha^{-1} yr^{-1} from 2003 to 2009. At the *Sphagnum* and *Eriophorum* sites, the annual GHG ranged from −806 to 377 and −849 to 1905 kg CO_2-eq. ha^{-1} yr^{-1}, respectively, and the corresponding means were −162 and 562 kg CO_2-eq. ha^{-1} yr^{-1}, respectively. Therefore, the modeled results demonstrated that the wetter *Eriophorum* site showed stronger warming potential in comparison with the dry *Palsa* site, although the *Eriophorum* site acted as a larger net C sink (Fig. 5b).

3.3 Possible changes of C fluxes due to permafrost thaw at Stordalen

Interpretation of aerial images of Stordalen showed that the area of “hummock” (*Palsa*) cover declined from 9.2 to 8.3 ha, while the area of “semiwet” and “wet” (*Sphagnum*) cover increased from 6.0 to 6.2 ha, and “tall graminoid” (*Eriophorum*) cover increased from 1.3 to 2.0 ha from 1970 to 2000 (Malmer et al., 2005; Johansson et al., 2006b). These changes in vegetation cover indicate a trend toward a wetter ecosystem probably as a direct consequence of permafrost thaw at Stordalen. Given that soil thaw rate accelerated under wet conditions (Fig. 2), this wetter trend may further accelerate permafrost degradation. By applying the modeled annual CO_2 and CH_4 fluxes to these areas changes, we estimated an increase of 578 kg C yr^{-1} (or 35 kg C ha^{-1} yr^{-1} for the study area of 16.5 ha) in CO_2 uptake and an increase of 79 kg C yr^{-1} (or 4.8 kg C ha^{-1} yr^{-1}) in CH_4 emission from 1970 to 2000 at Stordalen. Using a 100-year GWP value for methane, the net impact due to the vegetation change is a net CO_2 equivalent emission of 527 kg CO_2-eq. yr^{-1}; i.e., the warming impact of increased CH_4 emission more than offsets the cooling impact of increased CO_2 uptake at the mire.

4 Discussion

4.1 Validation of DNDC

In this study, we applied the new version of DNDC to simulate soil freeze/thaw dynamics and C fluxes across three typical land cover types (i.e., *Palsa*, *Sphagnum*, and *Eriophorum*) at Stordalen, Sweden, which are considered to represent different stages of permafrost thaw (Johansson et al., 2006b; Bäckstrand et al., 2010). Consistent with field measurements, DNDC simulated significant differences in C fluxes across these three land cover types. In addition, the model generally captured the magnitudes and temporal dynamics of soil thaw, NEE, and CH_4 fluxes (Figs. 2–4). The model validation suggests that the enhanced DNDC potentially can be used to predict impacts of permafrost thaw and subsequent changes in soil hydrology and vegetation on C dynamics in northern peatlands. However, we also note some discrepancies between the modeled results and the field measurements.

Compared to daily observations of NEE, DNDC overestimated CO_2 uptake rates (i.e., predicted lower NEE) on some days during growing seasons (Fig. 3), which may have resulted from over-prediction of photosynthesis. Because meteorological data at the ANS (10 km northwest of Stordalen) were used to support the simulations and photosynthesis is closely related to climate factors, deviations in predicting daily variability in photosynthesis may be caused by lacking site-specific data. Discrepancies between the modeled and observed NEE also appeared at the *Sphagnum* site in 2003 (Fig. 3h). Inconsistent with field data in other years, high net uptake rates of CO_2 occurred at this site during 25 May to 22 June in 2003 (Fig. 3h–n), even though solar radiation and air temperature were low (Fig. 1), causing DNDC to predict lower uptake rates. Further studies are needed to clarify the differences in seasonal characteristics of NEE between 2003 and other years, as well as the inconsistencies between the predictions and observations at the *Sphagnum* site in 2003.

As illustrated by Fig. 4, DNDC approximately matched the observed daily CH_4 fluxes at both the *Sphagnum* and *Eriophorum* sites, despite few inconsistencies (e.g., in 2003 at the *Sphagnum* site and in 2008 at the *Eriophorum* site). Model parameters for soil and vegetation characteristics were derived from a number of studies done at Stordalen since the International Biosphere Program in the early 1970s (Sonesson et al., 1980). Because these parameters have strong influences on soil climate, plant growth, and soil biogeochemistry in DNDC, potential biases in inputs could affect model results, including CH_4 fluxes. In addition, it should be noted that the modeled C fluxes over winter periods remain uncertain because observations utilized for model validation were primarily available during growing seasons. Further tests are necessary to verify the model's predictions of low C fluxes during winter periods.

Although the modeled C fluxes were tested against field measurements with encouraging results, we note that uncertainty may exist in simulating individual processes in C transformations. For example, methane flux is predicted by DNDC as the net result of CH_4 production, oxidation, and transport processes. Validating simulations of CH_4 emission against field measurements did not evaluate the DNDC's simulation of these three processes individually. One approach for testing/constraining simulation of the individual processes is to include stable isotopes and isotope fractionation during the processes of methanogenesis (acetate fermentation and CO_2 reduction), methane oxidation, and methane transport (e.g., Chanton et al., 2005; Corbett et al., 2013). This is planned for future model development.

4.2 Permafrost thaw and C fluxes

Our modeled results provide some indications on how C fluxes will change with ongoing permafrost thaw at Stordalen. If the *Palsa* evolves into *Sphagnum* or *Eriophorum* during permafrost thaw, the mire may be able to sequester more atmospheric C, considering the higher rates of net C uptake shown at the *Sphagnum* or *Eriophorum* sites (Fig. 5b). However, increases of net C uptake were positively correlated with increases of CH_4 emissions across the thaw gradient at Stordalen (Fig. 5), indicating that permafrost thaw will generate a tradeoff of GHG. If the net impact is calculated using the GWP methodology (e.g., Shine et al., 1990), the balance depends on the relative rate of changes in CO_2 uptake and CH_4 emissions and the time horizon chosen for the GWP calculation (e.g., Frolking and Roulet, 2007; Whiting and Chanton, 2001).

By applying the modeled C fluxes to the areal changes of land cover types at Stordalen, we estimated that the net impact due to the vegetation change is a net CO_2 equivalent emission of 527 kg CO_2-eq. yr^{-1} from 1970 to 2000 at Stordalen. Johansson et al. (2006b) also used a 100-year GWP value for methane, but treated their "wet" cover somewhat differently – equivalent to "semiwet" (*Sphagnum*) for NEE due to similarity in vegetation composition, but with a higher value for CH_4 emission as it was an inundated area. Because the "wet" area was nearly 30 % of the study region and expanded from 1970 to 2000, Johansson et al. (2006b) estimated that the mire was a GHG source in terms of CO_2 equivalents to the atmosphere, and they reported an increase of 47 % in net radiative forcing from 1970 to 2000 by considering the fluxes during growing season. Our analysis estimated that the mire was a GHG sink due to a lower value for CH_4 emission in "wet" areas, and yielded an overall decrease of 27 % in net radiative cooling from 1970 to 2000. The differences and uncertainties in these interpretations illustrate an important scaling challenge – how many land cover classes are needed and what are the most important distinctions to consider?

4.3 Modeling impacts of permafrost thaw on C fluxes

As a biogeochemical model with detailed C and N processes, DNDC has been widely applied to predict plant growth, soil C sequestration, and GHG emissions (e.g., Giltrap et al., 2010). However, the model lacked detailed processes simulating the soil thermal regime in permafrost areas, and did not describe impacts of permafrost dynamics on biogeochemistry. To correct these deficiencies, we incorporated NEST into DNDC. In the enhanced DNDC model, climate, land surface and soil environments (e.g., snow pack, soil thermal and permafrost regimes, soil moisture, substrates concentration), and transformations of C and N are closely linked. Therefore, the model should better serve to investigate impacts of climate change on C fluxes in high-latitude ecosystems.

Modeling impacts of permafrost thaw on C fluxes is in a very early stage, and much additional work is required for a more complete treatment to all of the processes involved. As shown in this and other studies (e.g., Olefeldt et al., 2013), NEE and CH_4 fluxes are strongly controlled by soil water regime and vegetation characteristics, which stresses the importance of considering changes in soil hydrology and vegetation when predict responses of C turnover to climate change in permafrost ecosystems. Although changes in wetland cover and vegetation have been observed along with permafrost degradation in northern peatlands (e.g., Goetz et al., 2011; Smith et al., 2005), most modeling work that predicts impacts of climate change on C turnover are based on static distribution of wetlands and vegetation (Bohn and Lettenmaier, 2010). Therefore biases may result from neglecting changes in water table regime and vegetation transitions along with permafrost thaw. In this study, we determined different soil water conditions for the three land cover types at Stordalen by combining the observed WTD and the hydrological module of DNDC. The required hydrological parameters were estimated by calibrating against WTD datasets (Table 1). While these parameters were empirically determined, they are consistent with the general topography of Stordalen, with the *Palsa* surface elevated 0.5–2.0 m above the *Eriophorum* surface, and the *Sphagnum* surface at intermediate elevation (Olefeldt and Roulet, 2012). However, it should be noted that sufficient WTD data are required for calibrating these hydrological parameters if the model is to be applied to other peatlands. Although different WTD and vegetation characteristics were used as inputs for different land cover types to represent changes in soil water regime and vegetation along with permafrost thaw at Stordalen, it would be ideal to incorporate these changes dynamically into the model's framework for better understanding how permafrost thaw affect landscape wetness and how this in turn affect vegetation and C fluxes.

5 Conclusions

Climate warming and associated permafrost degradation are expected to have significant impacts on the C balance of permafrost ecosystems but the magnitude is uncertain. We incorporated a permafrost model, NEST, into a biogeochemical model, DNDC, to model C dynamics in high-latitude ecosystems. The enhanced DNDC model was applied to assess effects of permafrost thaw on C fluxes of a sub-arctic peatland at Stordalen, Sweden. DNDC simulated soil freeze/thaw dynamics and C fluxes across three typical land cover types (i.e., *Palsa*, *Sphagnum*, and *Eriophorum*) at Stordalen, which span a gradient in the processes of permafrost thaw. Model results were tested against multi-year field measurements. The model validation indicates that DNDC was able to capture differences in soil thaw, NEE, and CH_4 fluxes across the *Palsa*, *Sphagnum*, and *Eriophorum* sites at Stordalen. In addition, the simulated magnitudes and temporal dynamics of soil thaw, NEE, and CH_4 fluxes were in general agreement with field measurements. Consistent with the results from field studies, the modeled C fluxes across permafrost thaw gradient demonstrate that permafrost thaw and the associated changes in soil hydrology and vegetation increase net uptake of C from atmosphere, but also increase the radiative forcing impacts on climate due to increased CH_4 emission. By using the modeled annual C fluxes and reported areas of vegetation cover in 1970 and 2000, we estimated that the Stordalen mire was a net GHG sink (using a 100-year GWP value for methane) and yielded an overall decrease of 27 % in net radiative cooling from 1970 to 2000.

Acknowledgements. This study was supported by the NASA Terrestrial Ecology Program (NNX09AQ36G), the US Department of Energy (DE-SC0004632), and the US National Science Foundation (ARC-1021300). We thank the Abisko Scientific Research Station for providing the meteorological data.

References

ACIA: Arctic Climate Impact Assessment: Scientific Report, Cambridge University Press, New York, 2005.

Aerts, R., Wallén, B., and Malmer, N.: Growth-limiting nutrients in *Sphagnum*-dominated bogs subject to low and high atmospheric nitrogen supply, J. Ecol., 80, 131–140, 1992.

Aerts, R., Wallén, B., Malmer, N., and de Caluwe, H.: Nutritional constraints on *Sphagnum*-growth and potential decay in northern peatlands, J. Ecol., 89, 292–299, 2001.

Avis, C. A., Weaver, A. J., and Meissner, K. J.: Reduction in areal extent of high-latitude wetlands in response to permafrost thaw, Nat. Geosci., 4, 444–448, 2011.

Åkerman, H. J. and Johansson, M.: Thawing permafrost and thicker active layers in sub-arctic Sweden, Permafrost Periglac., 19, 279–292, 2008.

Bäckstrand, K., Crill, P. M., Mastepanov, M., Christensen, T. R., and Bastviken, D.: Total hydrocarbon flux dynamics at a subarctic mire in northern Sweden, J. Geophys. Res., 113, G03026, doi:10.1029/2008JG000703, 2008.

Bäckstrand, K., Crill, P. M., Jackowicz-Korczyñski, M., Mastepanov, M., Christensen, T. R., and Bastviken, D.: Annual carbon gas budget for a subarctic peatland, Northern Sweden, Biogeosciences, 7, 95–108, doi:10.5194/bg-7-95-2010, 2010.

Bohn, T. J. and Lettenmaier, D. P.: Systematic biases in large-scale estimates of wetland methane emissions arising from water table formulations, Geophys. Res. Lett., 37, L22401, doi:10.1029/2010GL045450, 2010.

Callaghan, T. V., Bergholm, F., Christensen, T. R., Jonasson, C., Kokfelt, U., and Johansson, M.: A new climate era in the sub-Arctic: accelerating climate changes and multiple impacts, Geophys. Res. Lett., 37, L14705, doi:10.1029/2009GL042064, 2010.

Chanton, J. P., Chasar, L., Glaser, P. H., and Siegel, D. I.: Carbon and hydrogen isotopic effects in microbial methane from terrestrial environments, in: Stable Isotopes and Biosphere-Atmosphere Interactions: Processes and Biological Controls, edited by: Flanagan, L. B., Ehleringer, J. R., and Pataki, D. E., Elsevier, Amsterdam, 85–105, 2005.

Christensen, T. R., Johansson, T., Åkerman, H. J., Mastepanov, M., Malmer, N., Friborg, T., Crill, P., and Svensson, B. H.: Thawing sub-arctic permafrost: effects on vegetation and methane emissions, Geophys. Res. Lett., 31, L04501, doi:10.1029/2003GL018680, 2004.

Clauser, C. and Huenges, E.: Thermal conductivity of rocks and minerals, in: Rock Physics & Phase Relations: a Handbook of Physical Constants, edited by: Ahrens, T. J., AGU, Washington DC, 105–126, 1995.

Corbett, J. E., Tfaily, M. M., Burdige, D. J., Cooper, W. T., Glaser, P. H., and Chanton, J. P.: Partitioning pathways of CO_2 production in peatlands with stable carbon isotopes, Biogeochemistry, 114, 327–340, doi:10.1007/s10533-012-9813-1, 2013.

Dorrepaal, E., Toet, S., van Logtestijn, R. S. P., Swart, E., van de Weg, M. J., Callaghan, T. V., and Aerts, R.: Carbon respiration from subsurface peat accelerated by climate warming in the subarctic, Nature, 460, 616–619, 2009.

Frolking, S. and Roulet, N. T.: Holocene radiative forcing impact of northern peatland carbon accumulation and methane emissions, Glob. Change Biol., 13, 1079–1088, 2007.

Frolking, S., Talbot, J., Jones, M., Treat, C. C., Kauffman, J. B., Tuittila, E. S., and Roulet, N. T.: Peatlands in the Earth's 21st century climate system, Environ. Rev., 19, 371–396, 2011.

Fumoto, F., Kobayashi, K., Li, C., Yagi, K., and Hasegawa, T.: Revising a process-based biogeochemistry model (DNDC) to simulate methane emission from rice paddy fields under various residue management and fertilizer regimes, Glob. Change Biol., 14, 382–402, 2008.

Giltrap, D. L., Li, C., and Saggar, S.: DNDC: a process-based model of greenhouse gas fluxes from agricultural soils, Agr. Ecosyst. Environ., 136, 292–230, 2010.

Goetz, S. J., Epstein, H. E., Bhatt, U. S., Jia, G. J., Kaplan, J. O., Lischke, H., Yu, Q., Bunn, A., Lloyd, A. H., Alcaraz-Segura, D., Beck, P. S. A., Comiso, J. C., Raynolds, M. K., and Walker, D. A.: Recent changes in arctic vegetation: satellite observations and simulation model predictions, in: Eurasian Arctic Land Cover and Land Use in a Changing Climate, edited by: Gutman, G. and Reissell, A., Springer, Nertherlands, 9–36, 2011.

IPCC: Climate change 2007: the physical science basis, in: Contribution of Working Group I to the Fourth Assessment Report of the Intergovernmental Panel on Climate Change: "The

Physical Science Basis", edited by: Solomon, S., Qin, D., Manning, M., Chen, Z., Marquis, M., Averyt, K. B., Tignor, M., and Miller, H. L., Cambridge University Press, Cambridge, 2007.

Jackowicz-Korczyñski, M., Christensen, T. R., Bäckstrand, K., Crill, P. M., Friborg, T., Mastepanov, M., and Ström, L.: Annual cycle of methane emission from a subarctic peatland, J. Geophys. Res., 115, G02009, doi:10.1029/2008JG000913, 2010.

Johansson, M., Christensen, T. R., Åkerman, J. H., and Callaghan, T. V.: What determines the current presence or absence of permafrost in the torneträsk region, a sub-arctic landscape in northern Sweden, Ambio, 35, 190–197, 2006a.

Johansson, T., Malmer, N., Crill, P. M., Friborg, T., Åkerman, J., Mastepanov, M., and Christensen, T. R.: Decadal vegetation changes in a northern peatland, greenhouse gas fluxes and net radiative forcing, Glob. Change Biol., 12, 2352–2369, doi:10.1111/j.1365-2486.2006.01267.x, 2006b.

Kirschke, S., Bousquet, P., Ciais, P., Saunois, M., Canadell, J. G., Dlugokencky, E. J., Bergamaschi, P., Bergmann, D., Blake, D. R., Bruhwiler, L., Cameron-Smith, P., Castaldi, S., Chevallier, F., Feng, L., Fraser, A., Heimann, M., Hodson, E. L., Houweling, S., Josse, B., Fraser, P. J., Krummel, P. B., Lamarque, J., Langenfelds, R. L., Le Quere, C., Naik, V., O'Doherty, S., Palmer, P. I., Pison, I., Plummer, D., Poulter, B., Prinn, R. G., Rigby, M., Ringeval, B., Santini, M., Schmidt, M., Shindell, D. T., Simpson, I. J., Spahni, R., Steele, L. P., Strode, S. A., Sudo, K., Szopa, S., van der Werf, G. R., Voulgarakis, A., van Weele, M., Weiss, R. F., Williams, J. E., and Zeng, G.: Three decades of global methane sources and sinks, Nat. Geosci., 6, 813–823, doi:10.1038/NGEO1955, 2013.

Koven, C. D., Ringeval, B., Friedlingstein, P., Ciais, P., Cadule, P., Khvorostyanov, D., Krinner, G., and Tarnocai, C.: Permafrost carbon-climate feedbacks accelerate global warming, P. Natl. Acad. Sci. USA, 108, 14769–14774, 2011.

Li, C.: Modeling trace gas emissions from agricultural ecosystems, Nutr. Cycl. Agroecosys., 58, 259–276, doi:10.1023/A:1009859006242, 2000.

Li, C.: Quantifying greenhouse gas emissions from soils: scientific basis and modeling approach, Soil Sci. Plant Nutr., 53, 344–352, 2007.

Li, C., Frolking, S., and Frolking, T. A.: A model of nitrous oxide evolution from soil driven by rainfall events: 1. Model structure and sensitivity, J. Geophys. Res., 97, 9759–9776, 1992a.

Li, C., Frolking, S., and Frolking, T. A.: A model of nitrous oxide evolution from soil driven by rainfall events: 2. Model applications, J. Geophys. Res., 97, 9777–9783, 1992b.

Li, C., Aber, J., Stange, F., Butterbach-Bahl, K., and Papen, H.: A process-oriented model of N_2O and NO emissions from forest soils: 1. Model development, J. Geophys. Res., 105, 4365–4384, 2000.

Li, C., Salas, W., Zhang, R., Krauter, C., Rotz, A., and Mitloehner, F.: Manure-DNDC: a biogeochemical process model for quantifying greenhouse gas and ammonia emissions from livestock manure systems, Nutr. Cycl. Agroecosys., 93, 163–200, doi:10.1007/s10705-012-9507-z, 2012.

Lund, M., Lafleur, P. M., Roulet, N. T., Lindroth, A., Christensen, T. R., Aurela, M., Chojnicki, B. H., Flanagan, L. B., Humphreys, E. R., Laurila, T., Oechel, W. C., Olejnik, J., Rinne, J., Schubert, P., and Nilsson, M. B.: Variability in exchange of CO_2 across 12 northern peatland and tundra sites, Glob. Change Biol., 16, 2436–2448, 2010.

Majorowicz, J. and Wybraniec, S.: New terrestrial heat flow map of Europe after regional paleoclimatic correction application, Int. J. Earth Sci., 100, 881–887, 2011.

Malmer, N. and Wallén, B.: Peat formation and mass balance in subarctic ombrotrophic peatlands around Abisko, northern Scandinavia, Ecol. Bull., 45, 79–92, 1996.

Malmer, N., Johansson, T., Olsrud, M., and Christensen, T. R.: Vegetation, climatic changes and net carbon sequestration in a North-Scandinavian subarctic mire over 30 years, Glob. Change Biol., 11, 1895–1909, 2005.

McGuire, A. D., Anderson, L. G., Christensen, T. R., Dallimore, S., Guo, L., Hayes, D. J., Helmann, M., Lorenson, T. D., Macdonald, R. W., and Roulet, N.: Sensitivity of the carbon cycle in the Arctic to climate change, Ecol. Monogr., 79, 523–555, 2009.

Moriasi, D. N., Arnold, J. G., Van Liew, M. W., Bingner, R. L., Harmel, R. D., and Veith, T. L.: Model evaluation guidelines for systematic quantification of accuracy in watershed simulations, T. ASABE, 50, 885–900, 2007.

Nungesser, M. K.: Modelling microtopography in boreal peatlands: hummocks and hollows, Ecol. Model., 165, 175–207, 2003.

Olefeldt, D. and Roulet, N. T.: Effects of permafrost and hydrology on the composition and transport of dissolved organic carbon in a subarctic peatland complex, J. Geophys. Res., 117, G01005, doi:10.1029/2011JG001819, 2012.

Olefeldt, D., Roulet, N. T., Bergeron, O., Crill, P. M., Bäckstrand, K., and Christensen, T. R.: Net carbon accumulation of a high-latitude permafrost palsa mire similar to permafrost-free peatlands, Geophys. Res. Lett., 39, L03501, doi:10.1029/2011GL050355, 2012.

Olefeldt, D., Turetsky, M. R., Crill, P. M., and McGuire, A. D.: Environmental and physical controls on northern terrestrial methane emissions across permafrost zones, Glob. Change Biol., 19, 589–603, 2013.

Olsrud, M. and Christensen, T. R.: Carbon partitioning in a wet and a semiwet subarctic mire ecosystem based on in situ ^{14}C pulse-labelling, Soil Biol. Biochem., 43, 231–239, 2011.

Öquist, M. G. and Svensson, B. H.: Vascular plants as regulators of methane emissions from a subarctic mire ecosystem, J. Geophys. Res., 107, 4580, doi:10.1029/2001JD001030, 2002.

Payette, S., Delwaide, A., Caccianiga, M., and Beauchemin, M.: Accelerated thawing of subarctic peatland permafrost over the last 50 years, Geophys. Res. Lett., 31, L18208, doi:10.1029/2004GL020358, 2004.

Riseborough, D., Shiklomanov, N., Etzelmüller, B., Gruber, S., and Marchenko, S.: Recent Advances in Permafrost Modelling, Permafrost Periglac., 19, 137–156, 2008.

Rosswall, T., Flower-Ellis, J. G. K., Johansson, L. G., Jonsson, S., Rydén, B. E., and Sonesson, M.: Stordalen (Abisko), Sweden, Ecol. Bull., 20, 265–294, 1975.

Rydén, B. E. and Kostov, L.: Thawing and freezing in tundra soils, Ecol. Bull., 30, 251–281, 1980.

Rydén, B. E., Fors, L., and Kostov, L.: Physical properties of the tundra soil-water system at Stordalen, Abisko, Ecol. Bull., 30, 27–54, 1980.

Sachs, T., Giebels, M., Boike, J., and Kutzbach, L.: Environmental controls of CH_4 emission from polygonal tundra on the micro-site scale, Lena River Delta, Siberia, Glob. Change Biol., 16, 3096–3110, 2010.

Schneider von Deimling, T., Meinshausen, M., Levermann, A., Huber, V., Frieler, K., Lawrence, D. M., and Brovkin, V.: Estimating the near-surface permafrost-carbon feedback on global warming, Biogeosciences, 9, 649–665, doi:10.5194/bg-9-649-2012, 2012. checkCopernicus Publication!

Schuur, E. A. G., Bockheim, J., Canadell, J. G., Euskirchen, E., Field, C. B., Goryachkin, S. V., Hagemann, S., Kuhry, P., Lafleur, P. M., Lee, H., Mazhitova, G., Nelson, F. E., Rinke, A., Romanovsky, V. E., Shiklomanov, N., Tarnocai, C., Venevsky, S., Vogel, J. G., and Zimov, S. A.: Vulnerability of permafrost carbon to climate change: implications for the global carbon cycle, BioScience, 58, 701–714, 2008.

Schuur, E. A. G., Vogel, J. G., Grummer, K. G., Lee, H., Sickman, J. O., and Osterkamp, T. E.: The effect of permafrost thaw on old carbon release and net carbon exchange from tundra, Nature, 459, 556–559, 2009.

Schuur, E. A. G., Benjamin, A., and Permafrost Carbon Network: High risk of permafrost thaw, Nature, 480, 32–33, 2011.

Shine, K. P., Derwent, R. G., Wuebbles, D. F., and Morcrette, J. J.: Radiative forcing of climate, in: Climate Change: The IPCC Scientific Assessment, edited by: Houghton, J. T., Jenkins, G. J., and Ephraums, J. J., Cambridge University Press, Cambridge, UK, 41–68, 1990.

Smith, L. C., Sheng, Y., McDonald, G. M., and Hinzman, L. D.: Disappearing arctic lakes, Science, 308, 1429, doi:10.1126/science.1108142, 2005.

Sonneson, M., Jonsson, S., Rosswall, T., and Ryden, B. E.: The Swedish IBP/PT tundra biome project: objectives – planning – site, Ecol. Bull., 30, 7–25, 1980.

Stange, F., Butterbach-Bahl, K., Papen, H., Zechmeister-Boltenster, S., Li, C., and Aber, J.: A process-oriented model of N_2O and NO emissions from forest soils: 2. Sensitivity analysis and validation, J. Geophys. Res., 105, 4385–4398, 2000.

Ström, L. and Christensen, T. R.: Below ground carbon turnover and greenhouse gas exchanges in a sub-arctic wetland, Soil Biol. Biochem., 39, 1689–1698, 2007.

Waelbroeck, C.: Climate-soil processes in the presence of permafrost: a systems modelling approach, Ecol. Model., 69, 185–225, 1993.

Wania, R., Ross, I., and Prentice, I. C.: Integrating peatlands and permafrost into a dynamic global vegetation model: 1. Evaluation and sensitivity of physical land surface processes, Global Biogeochem. Cy., 23, GB3014, doi:10.1029/2008GB003412, 2009a.

Wania, R., Ross, I., and Prentice, I. C.: Integrating peatlands and permafrost into a dynamic global vegetation model: 2. Evaluation and sensitivity of vegetation and carbon cycle processes, Global Biogeochem. Cy., 23, GB3015, doi:10.1029/2008GB003413, 2009b.

Whiting, G. J. and Chanton, J. P.: Greenhouse carbon balance of wetlands: methane emission vs. carbon sequestration, Tellus B, 53, 521–528, 2001.

Yu, Z., Loisel, J., Brosseau, D. P., Beilman, D. W., and Hunt, S. J.: Global peatland dynamics since the Last Glacial Maximum, Geophys. Res. Lett., 37, L13402, doi:10.1029/2010GL043584, 2010.

Zhang, Y., Li, C., Trettin, C. C., Li, H., and Sun, G.: An integrated model of soil, hydrology and vegetation for carbon dynamics in wetland ecosystems, Global Biogeochem. Cy., 16, 1061, doi:10.1029/2001GB001838, 2002.

Zhang, Y., Chen, W., and Cihlar, J.: A process-based model for quantifying the impact of climate change on permafrost thermal regimes, J. Geophys. Res., 108, 4695, doi:10.1029/2002JD003354, 2003.

Zhang, Y., Chen, W., Smith, S. L., Riseborough, D. W., and Cihlar, J.: Soil temperature in Canada during the twentieth century: complex responses to atmospheric climate change, J. Geophys. Res., 110, D03112, doi:10.1029/2004JD004910, 2005.

Zhang, Y., Sachs, T., Li, C., and Boike, J.: Upscaling methane fluxes from closed chambers to eddy covariance based on a permafrost biogeochemistry integrated model, Glob. Change Biol., 18, 1428–1440, doi:10.1111/j.1365-2486.2011.02587.x, 2012.

Zhang, Y., Wang, X., Fraser, R., Olthof, I., Chen, W., Mclennan, D., Ponomarenko, S., and Wu, W.: Modelling and mapping climate change impacts on permafrost at high spatial resolution for an Arctic region with complex terrain, The Cryosphere, 7, 1121–1137, doi:10.5194/tc-7-1121-2013, 2013.

Zhuang, Q., Romanovsk, V. E., and McGuire, A. D.: Incorporation of a permafrost model into a large-scale ecosystem model: evaluation of temporal and spatial scaling issues in simulating soil thermal dynamics, J. Geophys. Res., 106, 33649–33670, 2001.

Zhuang, Q., Melillo, J. M., Kicklighter, D. W., Prinn, R. G., McGuire, A. D., Steudler, P. A., Felzer, B. S., and Hu, S.: Methane fluxes between terrestrial ecosystems and the atmosphere at northern high latitudes during the past century: a retrospective analysis with a process-based biogeochemistry model, Global Biogeochem. Cy., 18, GB3010, doi:10.1029/2004GB002239, 2004.

Zhuang, Q., Melillo, J. M., Sarofim, M. C., Kicklighter, D. W., McGuire, A. D., Felzer, B. S., Sokolov, A., Prinn, R. G., Steudler, P. A., and Hu, S.: CO_2 and CH_4 exchanges between land ecosystems and the atmosphere in northern high latitudes over the 21st century, Geophys. Res. Lett., 33, L17403, doi:10.1029/2006GL026972, 2006.

Table 1. The hydrological parameters used for modeling lateral flows*.

Sites	SIR	SOD (m)	SOR	GOD (m)	GOR
Sphagnum	1.0	0	1.0	0.25	0.01
Eriophorum	2.0	−0.05	0.3	0.05	0.01

* SIR, surface inflow rate, as the fraction of rainfall (or water from snow melt) flowed into the site from its surroundings; SOD, surface outflow depth, the water table (WT) depth (positive for below-ground and negative for above-ground) above which surface lateral outflow occurs; SOR, surface outflow rate, as the fraction of WT above the SOD which will be lost as surface outflow per day; GOD, ground outflow depth, the deepest WT depth above which ground outflow occurs; GOR, ground outflow rate, as the fraction of WT above the GOD which will be lost as ground outflow per day. These hydrological parameters were determined by calibrating against datasets of water table depth.

Table 2. The physiological parameters used for simulating plant growth.

Sites	MP[a]	SRF[b]	C/N[c]	TDD[d]	WR[e]	Vascularity	NFI[f]
Palsa	1000	0.35/0.65	90	1500	100	0	1.0
Sphagnum	1200	0.7/0.3	90	1500	100	0	1.1
Eriophorum	2500	0.5/0.5	90	1500	100	1	1.5

[a] MP, the maximum productivity under optimum growing conditions (kg C ha^{-1}). The values were estimated from Rosswall et al. (1975), Malmer and Walleñ (1996), and Malmer et al. (2005).

[b] SRF, the shoot and root fractions. The values were estimated from Ström and Christensen (2007), Olsurd and Christensen (2011). Note that the vegetation at the *Sphagnum* site is not 100 % moss.

[c] C/N, carbon to nitrogen ration of the plant biomass. The values were estimated from Aerts et al. (1992, 2001).

[d] TDD, the required accumulative air temperature (unit: °) of those above a 0 ° threshold ($> 0°$) for full vegetation growth.

[e] WR, amount of water required by the plant (g water g^{-1} dry matter).

[f] NFI, index of biological nitrogen fixation.

Table 3. Comparison of the modeled (M) and observed (O) net ecosystem exchanges (NEE, in $\mathrm{kg\,C\,ha^{-1}}$) of CO_2 during growing periods at the *Palsa*, *Sphagnum*, and *Eriophorum* sites[a].

Year	*Palsa*			*Sphagnum*			*Eriophorum*		
	O[b]	M	RMSE[c]	O	M	RMSE	O	M	RMSE
2003	−330[264]	−414	25	−394[59]	−326	17	−1118[219]	−1078	4
2004	−241[269]	−265	10	−441[73]	−452	2	−815[449]	−870	7
2005	−338[369]	−347	3	−525[69]	−521	1	−741[450]	−980	32
2006	−386[283]	−319	17	−356[27]	−330	8	−1034[94]	−1019	1
2007	−338[187]	−353	4	−436[114]	−424	3	−930[208]	−980	5
2008	−399[263]	−328	18	−264[79]	−288	9	−471[76]	−571	21
2009	−435[129]	−380	13	−212[75]	−203	4	−270[59]	−365	35

[a] The growing period in this study is defined as the periods during which measurements of continuous net CO_2 uptake were available. To calculate the total NEE over the growing period in each year, fluxes for the days lacking measurements were determined using the arithmetic mean fluxes of the two closest days when observations were performed. Daily fluxes from either direct measurements or gap-filling were then summed up to calculate the periodically cumulative NEE.

[b] Each figure number within the bracket is the standard deviation of three (*Palsa* and *Sphagnum*) or two (*Eriophorum*) replicate auto-chamber plots.

[c] RMSE, root mean squared error, %.

Title Page
Abstract | Introduction
Conclusions | References
Tables | Figures
◀| |▶
◀ ▶
Back | Close
Full Screen / Esc
Printer-friendly Version
Interactive Discussion

Table 4. Comparison of the modeled (M) and observed (O) CH_4 fluxes (in $kg\,C\,ha^{-1}$) during six study periods at the *Sphagnum* and *Eriophorum* sites[a].

Year	*Sphagnum*			*Eriophorum*		
	O[b]	M	RMSE[c]	O	M	RMSE
2003	17.2[5.2]	12.2	29	91.8[10.5]	76.4	17
2004	30.6[8.0]	24.3	21	121[14.7]	105	13
2005	25.1[4.7]	24.1	4	108[60.6]	101	7
2007	30.4[7.5]	35.7	18	116[22.2]	113	3
2008	9.7[4.2]	13.1	35	57.9[4.42]	45.3	22
2009	23.2[7.5]	27.5	18	111[21.7]	101	9

[a] The study period is the span during which continuous measurements of daily CH_4 fluxes were available. To calculate the total CH_4 emissions over the sampling period in each year, fluxes for the days lacking measurements were determined using the arithmetic mean fluxes of the two closest days when observations were performed. Daily fluxes from either direct measurements or gap-filling were then summed up to calculate the periodically cumulative CH_4 emissions.

[b] Each figure number within the bracket is the standard deviation of three (*Sphagnum*) or two (*Eriophorum*) replicate auto-chamber plots.

[c] RMSE, root mean squared error, %.

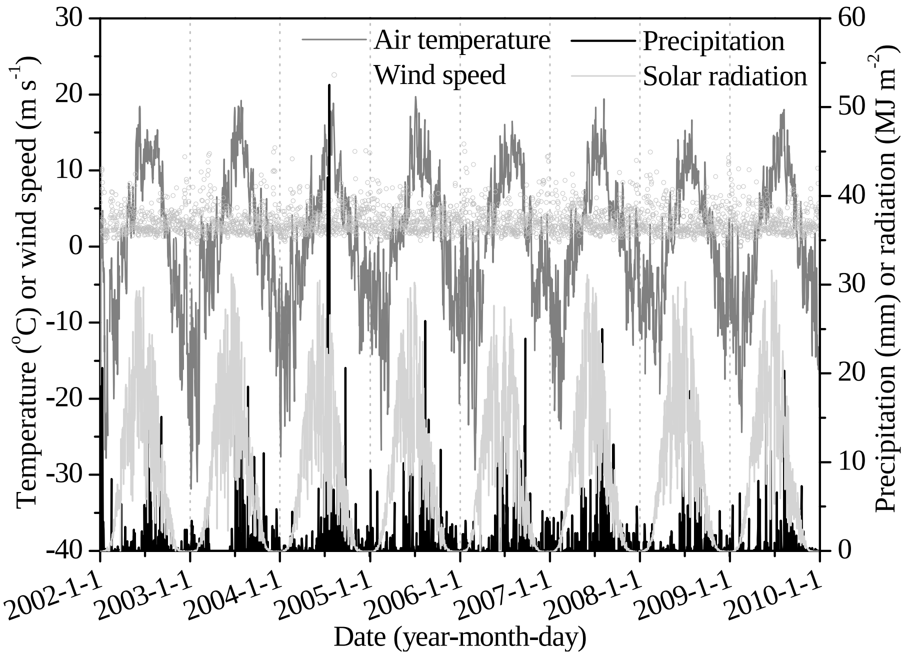

Fig. 1. Daily average air temperature, wind speed, precipitation, and solar radiation during 2002 to 2009. Data were recorded at the Abisko Scientific Research Station.

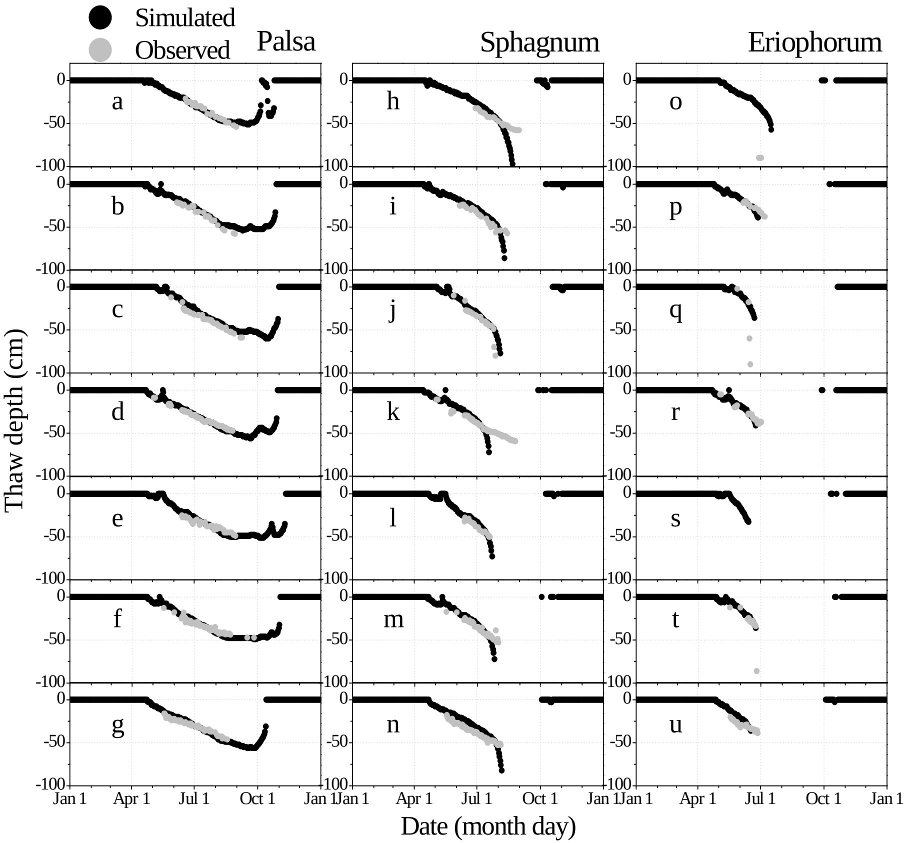

Fig. 2. Simulated and observed seasonal dynamics of thaw depth at the *Palsa* (**a** to **g**), *Sphagnum* (**h** to **n**), and *Eriophorum* (**o** to **u**) sites during 2003 to 2009. The entire soil layer was thawed at the beginning of field observations (in mid June) at the *Eriophorum* site in 2007 (panel **s**).

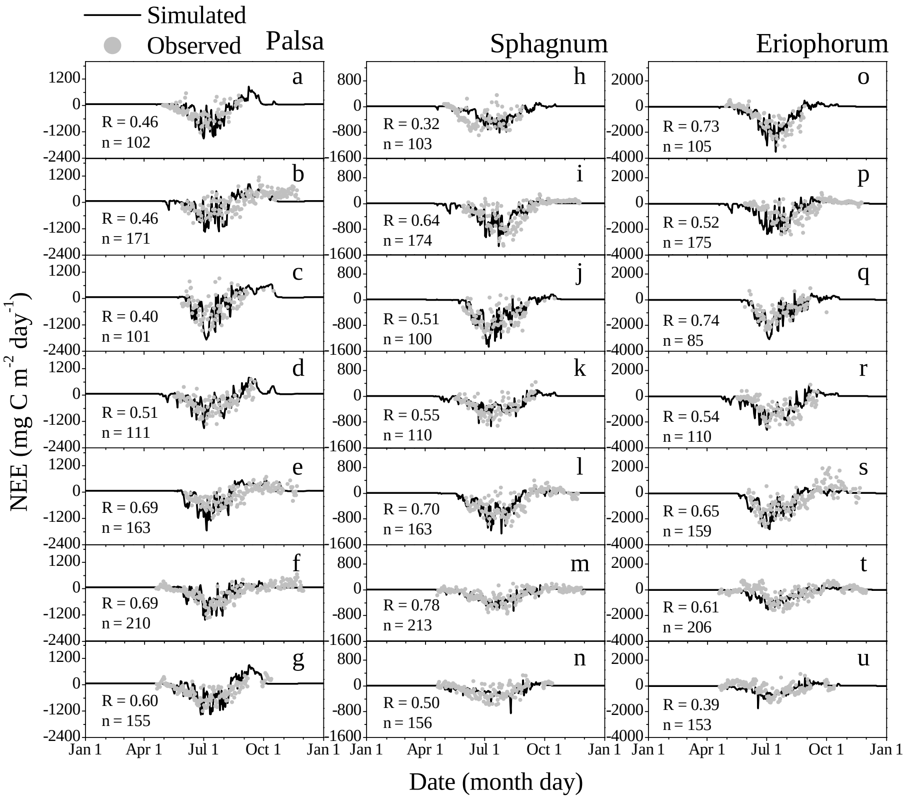

Fig. 3. Simulated and observed daily net ecosystem exchange (NEE) of CO_2 (mg C m^{-2} day^{-1}) at the *Palsa* (**a** to **g**), *Sphagnum* (**h** to **n**), and *Eriophorum* (**o** to **u**) sites during 2003 to 2009. The correlations between the simulated and observed daily NEE were significant for all cases ($P < 0.0001$, except for panel **i**, where $P < 0.001$). The observed data are the means of three (*Palsa* and *Sphagnum*) or two (*Eriophorum*) replicates and standard deviations are not shown for reasons of clarity. Note that scales of the vertical axis for NEE are different across the three sites.

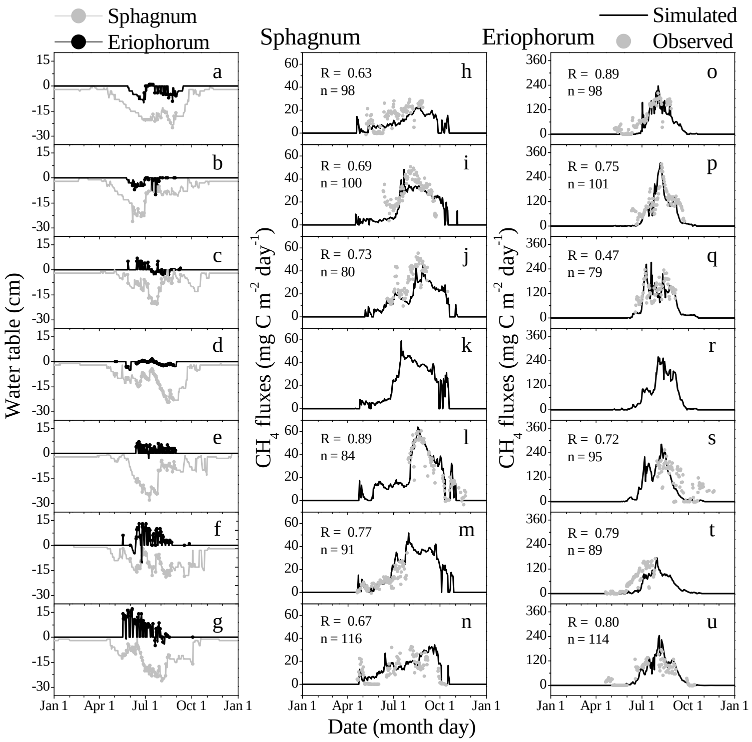

Fig. 4. Water table dynamics (**a** to **g**), simulated and observed daily CH_4 fluxes (mg C m^{-2} day^{-1}) at the *Sphagnum* (**h** to **n**) and *Eriophorum* (**o** to **u**) sites during 2003 to 2009. The correlations between the simulated and observed daily CH_4 fluxes were significant for all cases ($P < 0.0001$). The observed CH_4 fluxes are the means of three (*Sphagnum*) or two (*Eriophorum*) replicates and standard deviations are not shown for reasons of clarity. Because of instrument problems (Bäckstrand et al., 2008), observed data were not used for model evaluation in 2006. Note that scales of the vertical axis for CH_4 fluxes are different between the two sites.

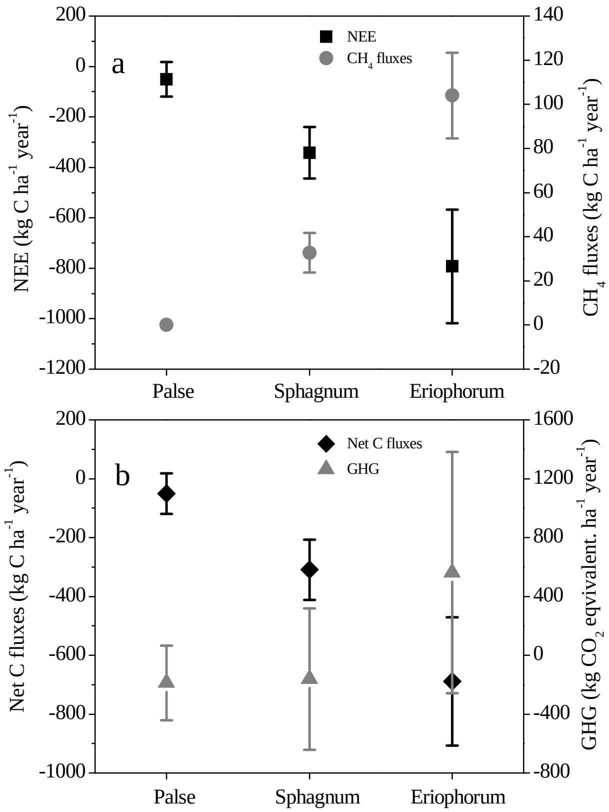

Fig. 5. Simulated net ecosystem exchange (NEE) of CO_2, CH_4 fluxes, net carbon fluxes, and net emissions of greenhouse gases (GHG) at the *Palsa*, *Sphagnum*, and *Eriophorum* sites. The CH_4 fluxes from the dry *Palsa* site were assumed negligible (here 0), based on field observations. Data are means of annual total fluxes from 2003 to 2009. Vertical bars are standard deviations of annual total fluxes from 2003 to 2009 and indicate inter-annual variations of C gases fluxes.